MATERIALS SCIENCE

Testing the paradigm of an ideal glass transition: Dynamics of an ultrastable polymeric glass

Heedong Yoon* and Gregory B. McKenna†

A major challenge to understanding glass-forming materials is obtaining equilibrium data far below the laboratory glass transition temperature T_g. The challenge arises because it takes geologic aging times to achieve the equilibrium glassy state when temperatures are well below T_g. Here, we finesse this problem through measurements on an ultrastable amorphous Teflon with fictive temperature T_f near to its Kauzmann temperature T_K. In the window between T_f and T_g, the material has a lower molecular mobility than the equilibrium state because of its low specific volume and enthalpy. Our measurements show that the determined scaled relaxation times deviate strongly from the classical expectation of divergence of time scales at a finite temperature. The results challenge the view of an ideal glass transition at or near to T_K.

INTRODUCTION

Conventional glass is a nonequilibrium material made by rapid cooling from the equilibrium or the supercooled liquid states. The kinetic glass transition occurs because the volume or enthalpy of the glass formers deviates from the equilibrium values because of reduced molecular mobility with decreasing temperature such that the material cannot respond at the experimental time scale, e.g., cooling rate (*1*–*39*). Understanding the nature of the glass transition remains a major challenge (*1*–*5*, *35*, *36*) in condensed matter physics. Of particular interest are the questions related to the existence of an "ideal" glass transition, first postulated by Gibbs and DiMarzio (*21*) based on a lattice model and the finding that the configurational entropy went to zero at a temperature T_2 above absolute zero, leading to a thermodynamic resolution of the Kauzmann paradox that glass-forming systems seem to have entropies that extrapolate to negative values (*32*), and the temperature at which the liquid entropy becomes less than that of the crystal is often referred to as the Kauzmann temperature T_K. In a similar vein, the temperature dependence of the slow dynamics is observed to be super-Arrhenius in the equilibrium or supercooled liquid states and is frequently described with the Vogel-Fulcher-Tammann (VFT) equation (*29*–*31*).

$$\tau = \tau_0 \exp\left[\frac{B}{T - T_\infty}\right] \quad (1)$$

Here, τ is a characteristic time, τ_0 and B are material parameters, and T_∞ is the VFT temperature and corresponds to the point at which the dynamics (viscosity or relaxation time) diverge. We see that this point occurs at a finite temperature T_∞ above absolute zero kelvin. This finite temperature has also been associated with the Kauzmann temperature (T_K) (*32*), which is often related to the existence of an ideal glass transition. Although the VFT equation describes well the experimental and theoretical results in the temperature range above the T_g, in the supercooled liquid regime, the extrapolation to below the kinetic glass transition remains problematic (*1*–*5*, *35*, *36*). However, the observation that T_K and T_∞ have similar values in many instances has resulted in a view that the thermodynamic T_2 (thermodynamic second-order transition temperature and that is often related to T_K) (*21*) or T_g is related to the result that multiple theories have been proposed that give VFT type of behavior above and below the conventional T_g; hence, they give a finite temperature divergence of relaxation time or viscosity (*19*, *24*, *34*). At the same time, there are theoretical proposals that argue against the dynamics of the equilibrium or supercooled liquid diverging at an ideal glass transition temperature (*1*–*4*, *8*–*14*, *16*–*27*). A detailed discussion of the various theories is beyond the scope of the present work, and the reader is directed to the relevant references for further information (*1*–*4*, *8*–*14*, *16*–*19*, *19*–*27*, *35*, *36*). It remains a fundamental problem of the experimental science of glass-forming liquids to establish whether the dynamic divergence occurs above absolute zero because of the extremely long time scales required to reach equilibrium. Early works (*8*, *10*, *11*, *37*, *38*) were able to provide some evidence of deviations from the VFT type of behavior by aging materials into equilibrium for times of multiple weeks, but the works were not completely accepted in the community (*37*, *38*). These works, regardless, were still performed relatively close to the nominal glass temperature, and the issue is extremely difficult to experimentally resolve, as materials can require geological time scales to reach equilibrium well below the laboratory determined T_g (*3*, *4*, *7*, *9*, *12*, *25*). For example, in a recent work, Zhao *et al.* (*9*) used a fossil amber [20 million years (Ma) old] from the Dominican Republic to test the dynamics of super-Arrhenius behavior deep in the glassy state. By examining the dynamics in the window between the greatly reduced fictive temperature T_f and the T_g, they showed that upper bounds to the relaxation times deviated strongly from the classic VFT behavior below T_g for temperatures as much as 43.6 K below the nominal T_g. Attempts to expand that work with ambers as old as 230 Ma were unsuccessful because of chemical instabilities of the amber samples tested (*40*). This has also led to some concern in the community that the Dominican amber may also be problematic, although the work from McKenna and coworkers (*40*) argued for the stability of this material. Hence, to interrogate the equilibrium response further below the T_g requires other means than ancient ambers to finesse the geological time issue to obtain or create glasses of extremely low fictive temperature.

The recent work from Ediger and coworkers (*4*, *6*) has shown that physical vapor deposition (PVD) can be used to produce ultrastable glasses that are deep into the energy landscape (*4*, *6*). These ultrastable glasses have shown high kinetic stability, low fictive temperature, and

Department of Chemical Engineering, Whitacre College of Engineering, Texas Tech University, Lubbock, TX 79409-3121, USA.
*Present address: Department of Chemical and Biological Engineering, College of Engineering, Drexel University, Philadelphia, PA 19104, USA.
†Corresponding author. Email: greg.mckenna@ttu.edu

high density similar to that expected of extremely aged glasses (*4*, *6*). The technique allows the synthesis of "extremely aged glasses" in a relatively short laboratory time scale (*4*, *6*). The stable glasses reported in prior works have generally been produced using low–molecular weight organic materials (*4*, *6*, *7*) that are hard to handle in addition to being made in small quantities, thus limiting the measurements that can be made with them. Recently, we have shown that the vapor deposition technique can be extended to amorphous fluoropolymers, and we were able to produce a stable polymeric glass having extremely high kinetic stability, i.e., a very low fictive temperature relative to the glass transition temperature (*7*). In that work, an amorphous Teflon was pyrolyzed in vacuum to produce an ultrastable polymeric glass. The postulated mechanism was that the polymeric chains were cleaved upon pyrolysis and they repolymerized onto the substrate during the vacuum pyrolysis deposition (VPD) process (*7*). This ultrastable Teflon film showed very low T_f values depending on the deposition substrate temperature. The lowest T_f obtained was 57 K below the nominal glass transition temperature, which corresponded to a greater T_f reduction relative to T_g than previously reported for stable glasses and greater than the 43.6 K that had been obtained with the 20 Ma old amber. Of significance is that the T_f was close to T_K (*8*). This low T_f opens the opportunity to investigate the dynamics deep into the glassy state and close to the nominal ideal glass transition temperature.

It is also worth remarking here that, because of the kinetic nature of the glassy state, the fictive temperature alone does not establish the full range of possible kinetic stabilities. Hence, there could be other histories that create similar fictive temperature glasses but that have different "stabilities" (either greater or lesser). However, when the fictive temperature is very low, such as is the case here, the glasses have high kinetic stability. Furthermore, the important point of the present work is to determine the relaxation response in the temperature window between T_f and T_g, as this is in a region where the relaxation time is greater than the time that would be measured in the equilibrium state. Thus, the exact degree of kinetic stability is not important, but the fictive temperature itself is. Relevant references are (*1*–*7*, *9*, *14*, *15*, *33*).

Although the ultrastable Teflon film gives a new opportunity to obtain fictive temperatures close to T_K, the VPD method readily produces only extremely small sample quantities. For example, here, the deposition rate of the material is 0.1 nm/s, which implies 10,000 s or approximately 3 hours to produce a 1-μm thick film. For standard viscoelastic measurements, a typical sample dimension would be 2 to 3 mm in thickness (*9*). Thus, it is a challenge to perform traditional dynamic measurements on these small amounts of material (*4*). To overcome this issue, in the present work, we have used the Texas Tech University (TTU) nanobubble inflation technique (*41*, *42*) to measure the viscoelastic response of the ultrastable Teflon films in the deep glassy regime in order to test the temperature dependence of the dynamics in the upper bound conditions, i.e., over a range that includes T_f to T_g. Prior bubble inflation studies have successfully shown that viscoelastic properties can be measured with sample sizes ranging from nano- to micrograms (*41*, *42*). Thus, by adopting the advantages of this technique, we are able to investigate the dynamic behavior for ultrastable polymeric films in the upper bound regime for the dynamics where the volume and enthalpy are lower than those of the glass in the equilibrium state. Most prior studies (*1*, *3*, *5*, *8*, *10*, *11*) have investigated the equilibrium dynamic response of polymeric materials in the temperature regime

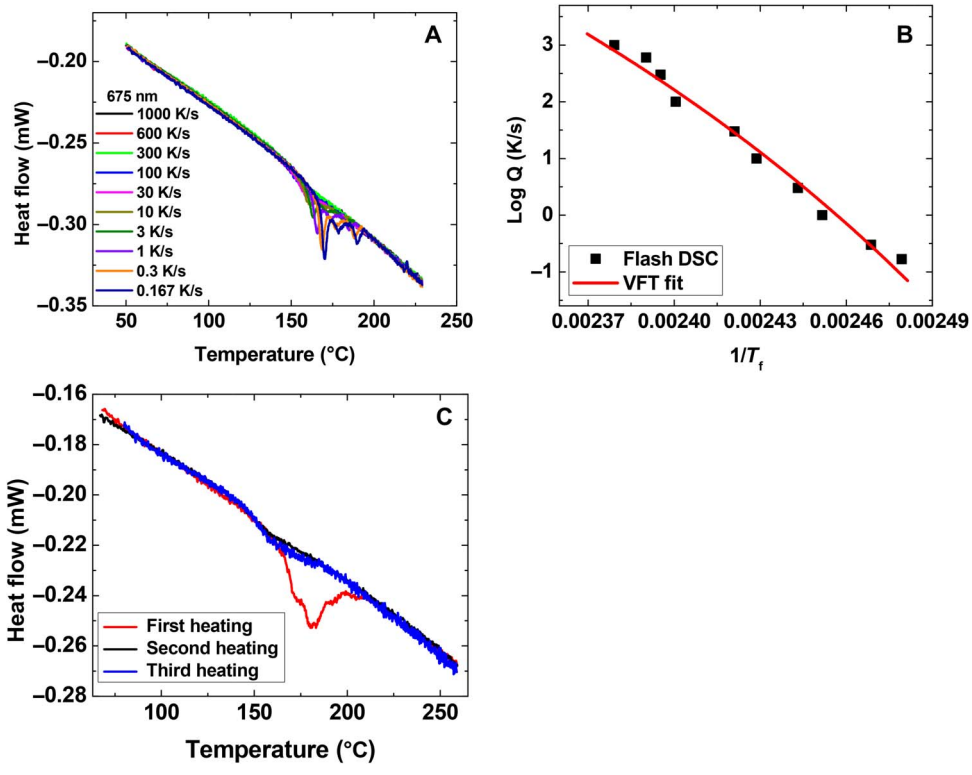

Fig. 1. Thermal signatures for an ultrastable amorphous Teflon. (**A**) Heat flow versus temperature for a 675-nm-thick VPD amorphous Teflon film at different cooling rates. (**B**) Logarithm of cooling rate versus $1/T_f$ and a VFT fit to the data. (**C**) Heat flow curve for a 300-nm VPD amorphous Teflon material deposited at 95°C. Images reproduced with permission from Yoon *et al.* (*7*). Copyright 2017 American Chemical Society.

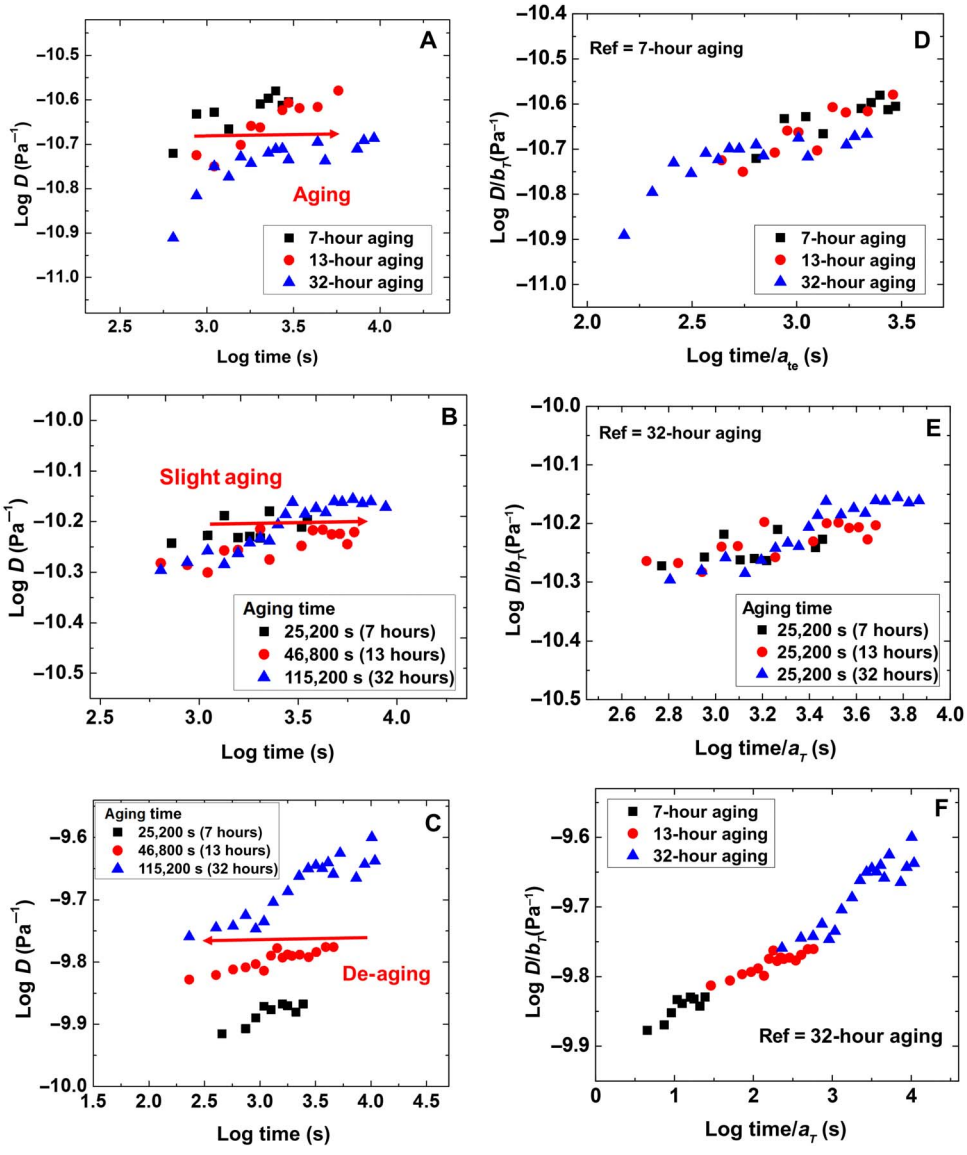

Fig. 2. Creep compliance curves for 110-nm stable amorphous Teflon films at different aging times. (**A**) 63°C, (**B**) 75°C, and (**C**) 90°C. (**D** to **F**) Creep master curves after applying time–aging time superposition to the data of (A) to (C).

close to T_g; however, to our knowledge, there are no such studies for temperatures in the deep glassy regime close to T_K. The 20 Ma old Dominican amber had a fictive temperature of 43.6 K below the T_g, which was approximately 27 K above the T_K (or T_∞) of the amber (*9*), nor are there reports of measurements of the viscoelastic response of ultrastable glasses in the deep glassy regime. In the following sections, we describe the ultrastable Teflon films and show results for the creep response at different aging times and temperatures deep in the glassy state.

As an additional consideration, one would like to be able to use the obtained data to discriminate among theoretical predictions of behavior below the nominal glass transition and, in this case, to temperatures near to the Kauzmann temperature. Therefore, we make comparisons of the results of the present experiments with the classic VFT extrapolations and with two theories from the literature that do not exhibit diverging time scales (*20*, *26*) with the intent to show that the methodology provides a viable means to differentiate among theories in addition to delving into the deviations from VFT behavior for the equilibrium glass far below the conventional glass temperature.

Heat flow responses for rejuvenated and stable amorphous Teflon films

In our prior work (*7*), we showed that ultrastable amorphous Teflon films can be produced by the VPD method. Figure 1A shows the heat flow curves for a 600-nm rejuvenated (heated above T_g and cooled before reheating) amorphous Teflon film measured by flash differential scanning calorimetry (DSC) for different cooling rates ranging from 1000 to 0.167 K/s. We see from Fig. 1A that the enthalpy peak increases with decreasing cooling rate. The T_f values of the rejuvenated Teflon films were calculated by the Moynihan equation (*14*). From a plot of logarithm of cooling rate versus $1/T_f$ (Fig. 1B), we see that T_f decreases with decreasing cooling rate. The T_f estimated at 0.167 K/s (10 K/min) was 403 K, and here, we remark that 403 K is used as the T_g

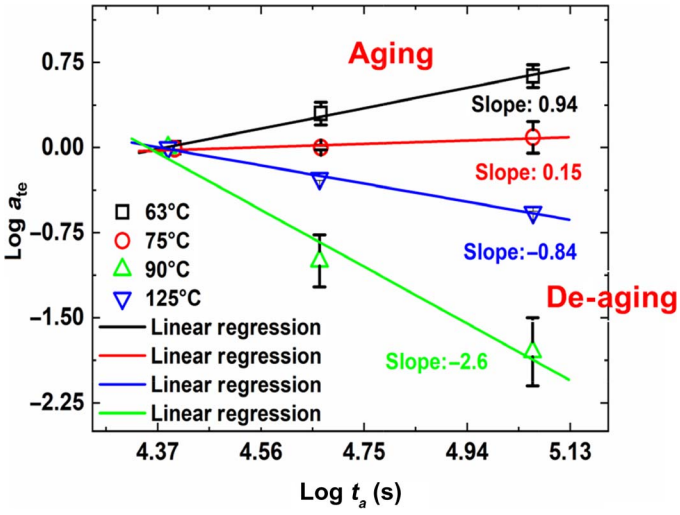

Fig. 3. Aging time dependence of the scaled relaxation times as log a_{te}. Aging regime represents "lower bound" response of the dynamics, while the de-aging regime represents "upper bound" response. Data indicate that the fictive temperature is slightly above 75°C.

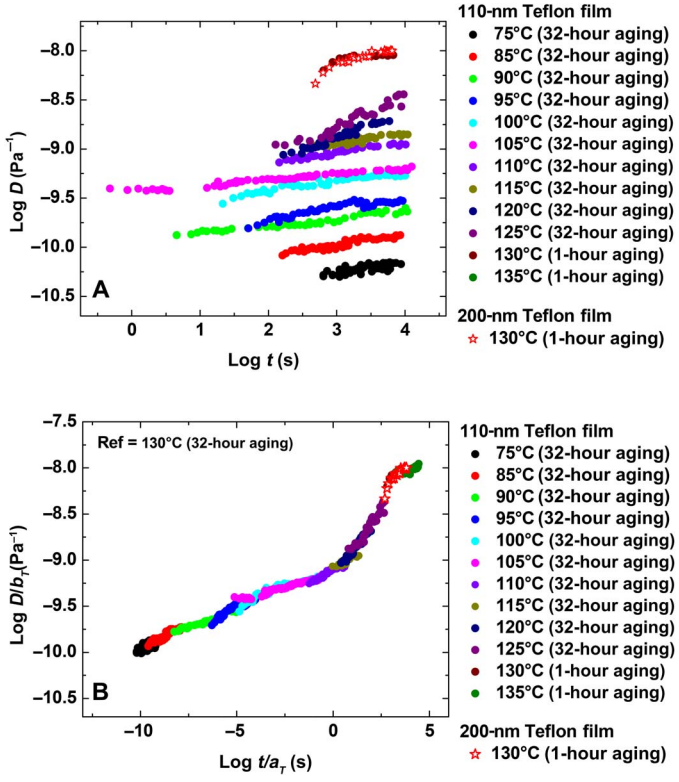

Fig. 4. Creep response of the ultrastable amorphous Teflon. (**A**) Creep compliance of 110-nm amorphous Teflon films at different temperatures after applying time–aging time superposition. (**B**) Creep master curve after applying time-temperature superposition to the data in (A).

for the amorphous Teflon films throughout this article. The VFT equation was fitted to T_f over different cooling rates, and the parameters obtained were as follows: log A = 16 ± 1, B = 2261 ± 103 K, and T_∞ = 346 ± 2 K, respectively (*7*). As already mentioned, T_K is often associated with T_∞; thus, here, we assumed $T_\infty = T_K$. Figure 1C shows the heat flow response for a 300-nm stable Teflon film deposited onto a substrate having a temperature of 95°C (0.91 T_g). We see that the first heating scan shows a very large enthalpy overshoot typical of ultrastable PVD-formed glasses (*5*, *7*) and larger than typical of conventionally aged glasses (*1*, *9*). This enthalpy peak disappears in the second heating scan, indicating that the material has devitrificated and returned to the thermally rejuvenated condition of a normal glass. The T_f reduction was calculated from the enthalpy difference between stable and rejuvenated conditions, as detailed in the prior work (*7*). The T_f for the ultrastable Teflon film deposited at 95°C was 349 K. This value is only 3 K higher than T_K (346 K). The sample used for the bubble inflation measurements was deposited on a substrate held at 0.85 T_g = 342.7 K = 69.5° C. The fictive temperature of this ultrastable glass was 348.2 K (75°C), which is 55 K below the T_g, viz., only 2.2 K above T_K.

Creep responses for ultrastable Teflon films

Determination of the creep response of the films allows us to establish the regime of aging or de-aging of the ultrastable Teflon as a function of temperature. Below T_f, the samples should age, i.e., the creep response should shift to longer times. When $T > T_f$, the creep response should shift to shorter times as aging time increases, i.e., the sample should devitrify. Figure 2 shows the creep compliance curves for 110-nm amorphous Teflon films for different aging times in the temperature range from T_f − 12°C to T_f + 15°C. In Fig. 2A, at 63°C (T_f − 12°C), the behavior should be that of the lower bound regime, and we observe "normal" aging behavior (*5*) as the creep compliance decreases or shifts to longer times with increasing aging time. At T_f (75°C), we observe a very weak aging behavior, indicating that the T_f estimated calorimetrically may be slightly higher than 75°C. In contrast to the response at 63°C, the creep compliance shows de-aging behavior at 90°C (T_f + 15°C), viz., the creep compliance increases and shifts to shorter times. The results observed for the aging and de-aging behaviors of the stable amorphous Teflon films are similar to prior observations from measurements on a 20 Ma old amber (*9*). Figure 2 (D to F) shows the creep master curves after applying time–aging time superposition to the data of Fig. 2 (A to C). Of interest here is how the creep response of ultrastable VPD Teflon differs from that of the thermally rejuvenated material, i.e., that heated above the glass transition, cooled to below the T_g, and tested as in conventional physical aging conditions (*5*). Figure S2 compares time–aging time master curve results for the stable and rejuvenated creep compliance behaviors at 105°C after 32 hours of aging ($t_{e,Ref}$ = 32 hours). We observe that the creep compliance master curve for the rejuvenated Teflon films is shifted to shorter times and is higher than that of the VPD stable Teflon film. Since the rejuvenated sample has a higher than equilibrium volume and enthalpy, while the ultrastable sample has lower than equilibrium volume and enthalpy, one would anticipate that the equilibrium value of the creep compliance curve will be between creep compliance curves for rejuvenated and VPD Teflon.

To further examine the dynamic behavior, we plotted the time–aging time shift factors applied in Fig. 2 as a function of the aging time in Fig. 3. At 63°C (in the lower bound regime), the relaxation time increases with increasing aging time. The slope for the log of the time–aging time shift factor versus log aging time (shift rate) (*5*) is 0.94. At $T = T_f$, the value of the slope decreases and becomes close to zero. This behavior is typical of normal aging where $T < T_f$ (*5*). On the other hand, in the upper bound regime ($T_f < T < T_g$), the relaxation time decreases with increasing aging time, showing a devitrification process (*9*). This is similar to what would be expected in up-jump aging experiments where

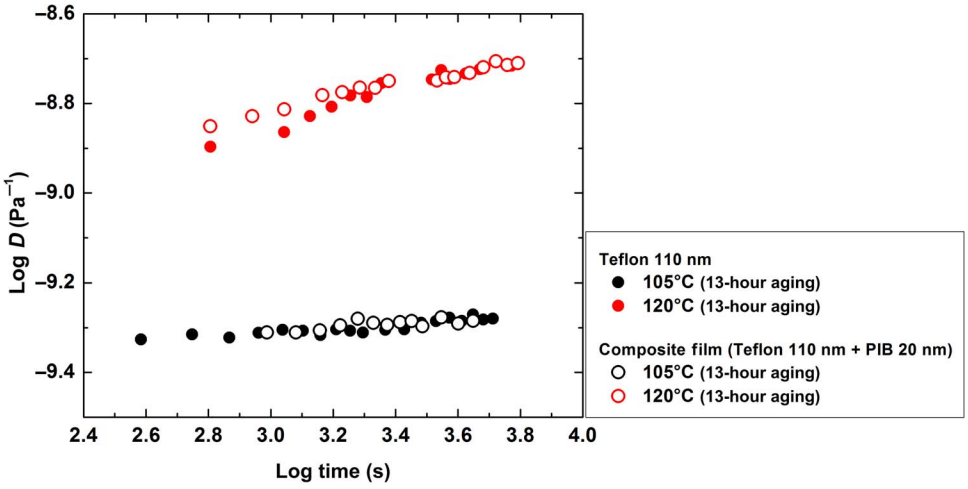

Fig. 5. Comparison of creep responses of 110-nm and 110-nm/20-nm bilayer films. Double logarithmic representation of the creep compliance versus log time for 110- and 130-nm composite bilayer films at 105° and 120°C, showing that the freestanding film and the supported film show the same response.

volume or enthalpy is below the equilibrium values (*9*, *33*). The slope values for the time–aging time shift factors at 90° and 125°C were −2.6 and −0.84, respectively.

The time–aging time master curves, all taken at the largest aging or de-aging time at each temperature, were superimposed using time-temperature superposition to form a single master curve, as shown in Fig. 4B. These shift factors are scaled relaxation times (*3*), viz., $a_T = \frac{\tau}{\tau_{ref}}$. We note that the logarithm of the compliance (−8.0) measured above T_g (at the longest reduced times in Fig. 4B) is lower than the reported macroscopic value (−6.33) (*43*). This behavior is similar to prior observations of rubber-like stiffening seen (*42*) in bubble inflation measurements on ultrathin films of several polymeric materials. McKenna and coworkers (*41*, *42*) observed that the compliance decreased as the film thickness decreased, and they interpreted this behavior as being due to the separation of α relaxation and Rouse mode caused by nanoconfinement effects. This is important because it is also known that nanoconfinement effects can sometimes, although not always, change the temperature dependence of the dynamics (*41*, *42*, *44*).

The purpose of the present work was to determine the macroscopic dynamic response for ultrastable amorphous Teflon films; therefore, we needed to carry out additional experiments to assure ourselves that the observed rubbery stiffening is not an evidence of a change in the temperature dependence of the dynamics in the 110-nm film studied here. To investigate this possibility, we performed additional creep experiments for two cases. First, we used a 200-nm single-layer ultrastable Teflon film for the creep experiments, and second, we used a bilayer composite film in which a 110-nm Teflon film was supported on a 20-nm poly (isobutylene) (PIB) film. The results were compared with those for the 110-nm single-layer freestanding film. Increasing the film thickness has the effect of showing that one is at the macroscopic limit of the creep response, i.e., there is no confinement effect on the glassy dynamics in the thin, freely standing film used in the present work. The aspect of using a bilayer composite film stems from the observation that confinement effects reported for ultrathin films supported on substrates generally are only seen below approximately 50 nm (*44*). Hence, two aspects of potential confinement effects on the results are directly addressed.

For the composite bilayer, we know the mechanical properties for nanometric thin PIB films from a recent bubble inflation study (*42*). In that work, the T_g for PIB was −73°C and the modulus measured for a 20-nm film at 23°C was 17 MPa. This is substantially smaller than that of the glassy amorphous Teflon, which we estimate from the bubble inflation experiments just reported for the different temperatures of interest. As outlined in section S2, we found that, for all temperatures, the error due to the PIB film on the measurement is less than 3%. Figure 5 compares the results from the creep compliance measurements for the 110-nm single-layer freestanding films to a 130-nm bilayer film at 105° and 120°C. We see that the creep compliance curves for the two cases are virtually the same. In addition, in Fig. 4, the creep compliance at 130°C for a freely standing 200-nm film is essentially the same as the response of the 110-nm films at 130°C. These results imply that although we observe rubbery stiffening behavior, the temperature dependence of the dynamics for the 110-nm freestanding Teflon films is not altered by nanoconfinement, i.e., the glassy dynamics are those of the macroscopic sample.

Comparison of the temperature dependence of the dynamics with the VFT extrapolation and two nondiverging models

To further investigate the dynamic behavior, we plotted the time-temperature shift factors obtained from the construction of the creep master curve in Fig. 6A as a function of T-T_g, where they are also compared with shift factors estimated from prior measurements of the cooling rate dependence of the fictive temperature for a 660-nm rejuvenated amorphous Teflon film (*7*). The results are also compared with dynamic shift factors reported for a 20 Ma old amber (*9*). In Fig. 6A, we see that the dynamic behavior for the ultrastable amorphous Teflon films in the temperature regime between T_f and T_g strongly deviates from the VFT behavior of the rejuvenated film. The region below T_g follows a close to Arrhenius temperature dependence, as shown in Fig. 6B. In addition, results from prior work (*9*) on a 20 Ma old amber are shown, and a nondiverging dynamic behavior was also observed in the upper bound regime between T_f and T_g. Extrapolating data from high temperature can cause uncertainties for determining the dynamic behavior. For instance, Ediger (*4*) estimated the relaxation time for an ultrastable indomethacin (IMC) by measuring transformation time into the supercooled liquid state. By extrapolating these data (Fig. 6B),

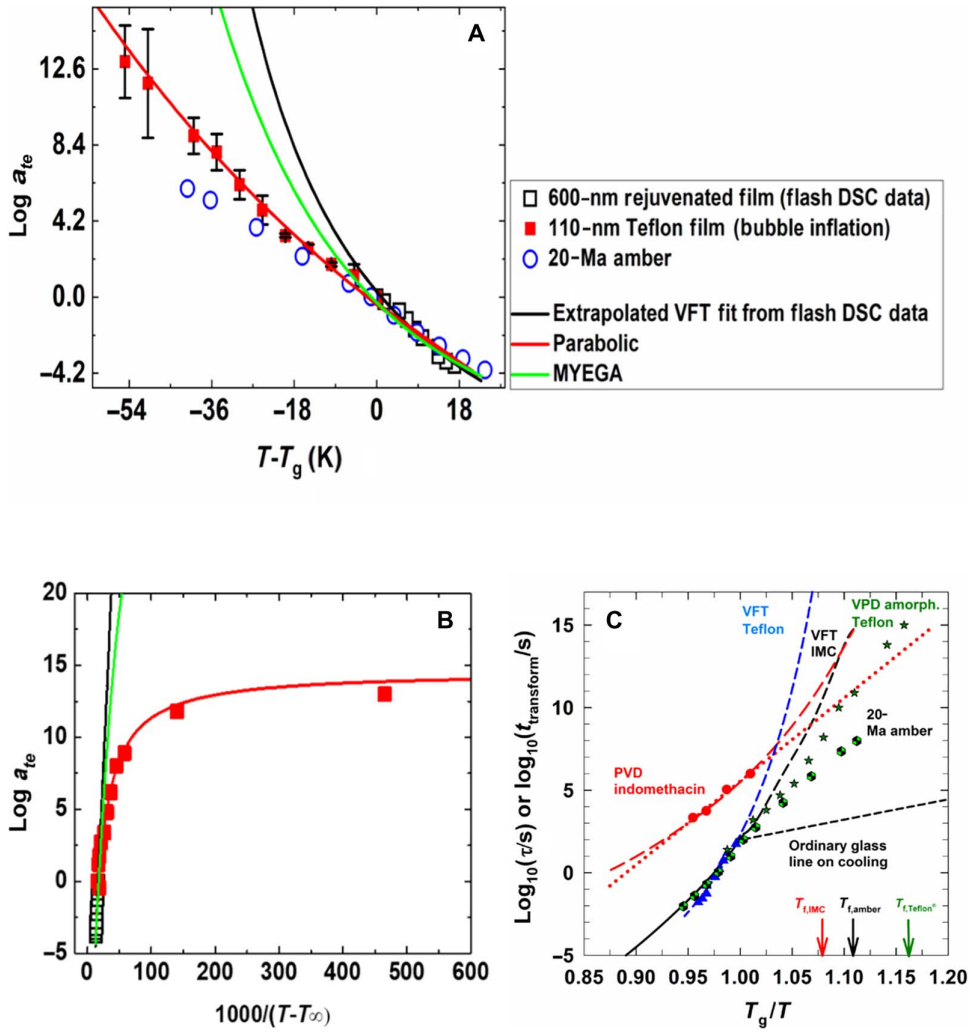

Fig. 6. Temperature dependence of the relaxation times, shift factors, a_T, or transformation times for the densified amorphous Teflon and other ultrastable glasses. (**A** and **B**) Time-temperature shift factors (scaled relaxation times) obtained from construction of master curve of Fig. 4 between T_f and to above T_g, i.e., in upper bound conditions for the amorphous Teflon. Also shown are results for a 20 Ma old amber (*9*). Presented as function of (A) T-T_g and (B) T-T_∞. For the amorphous Teflon, T_g determined by flash DSC and T_∞ determined from the VFT fit to flash DSC data of T_f as a function of cooling rate (*7*). (**C**) Temperature dependence of the relaxation time or the transformation time of ultrastable glasses versus T/T_g. Data for the IMC (solid circles, long dashed line, and dotted line) and "ordinary glass line" (black solid line and medium and small dashed lines) are from Ediger (*4*), whereas data for the 20 Ma old amber (hexagons) are from Zhao *et al*. (*9*). The amorphous Teflon data are for this study (stars and blue dashed line).

they estimated the dynamic behavior to be consistent with either the VFT or Arrhenius behavior as one goes below the conventional glass temperature (to higher values of T_g/T). The present method, however, eliminates the extrapolation for the temperatures between T_f and T_g, and Fig. 6B illustrates that the relaxation times for the ultrastable Teflon films and for the 20 Ma old amber (as estimated from the shift factors determined from time-temperature superpositioning of the data) deviate strongly from the VFT expression down to the reported fictive temperatures, which in the case of the amorphous Teflon is very close to the theoretical Kauzmann temperature T_K. It is worth noting that for the ultrastable glasses, the activation energy is still very high at 657 kJ/mol. This is higher than that of the 20 Ma old amber (435.8 kJ/mol), and both are typical of glass-forming liquids. A comment here is that the relaxation times estimated from the materials in the upper bound regime are for a nonequilibrium condition. The equilibrium relaxation times for the amorphous Teflon in the temperature range between T_f and T_g would be lower than those estimated here. Hence, the temperature dependence of the equilibrium relaxation times in this temperature regime may even more strongly deviate from the VFT behavior (*9*). It is also worth noting that at T_f, the relaxation time should be close to that of the equilibrium system (*1*–*3*, *8*–*11*); hence, the results here are possibly quite close to the actual equilibrium response. While there were some prior studies of equilibrium dynamics showing Arrhenius-like behavior below the T_g, these were limited to T_g–15°C or less (*1*, *3*, *5*, *8*, *10*, *11*). The upper bound type of experiment performed on the 20 Ma old amber extended this range to T_g–43.6°C, which was still 27°C above T_K. The present work on ultrastable Teflon films extends this temperature limit not only further below T_g (55°C) but also to the Kauzmann temperature T_K for the material. This large difference from T_g also presents the possibility not only to challenge the

VFT-type or ideal glass transition paradigms but also to use the data to differentiate among models that do not show divergence of the relaxation times at finite temperature (*1*, *3*, *16*–*27*, *29*–*34*). Here, we examine these two models: the so-called MYEGA model from Mauro *et al.* (*20*) and the parabolic model from Chandler and coworkers (*26*).

The temperature dependence of the dynamics in the MYEGA model (*20*) can be expressed as

$$\log a_T = \left(\frac{\tau}{\tau_{\text{ref}}}\right) = \frac{K}{T}\exp\left(\frac{C}{T}\right) + A \qquad (2)$$

where K, C, and A are fitting parameters, and T is the temperature. As noted previously, the temperature shift factors (a_T) can be thought of as scaled relaxation times (*3*). In the case of the parabolic model, the temperature dependence of a_T is given by (*26*)

$$\log a_T = \left(\frac{\tau}{\tau_{\text{ref}}}\right) = \left(\frac{J}{T_0}\right)^2\left(\frac{T_0}{T} - 1\right)^2 + DT_0 > T > T_x \qquad (3)$$

where J, T_0, and D are fitting parameters, and T_x is a temperature at which the relaxation time changes from VFT to Arrhenius-like behavior. The T_x was determined from fitting the parabolic and Arrhenius equations over different temperature ranges to obtain the smallest residuals. The T_x determined from the fitting was 130°C, which is the same as the calorimetric T_g for the material, similar to results from the 20 Ma old amber. In Fig. 6, we see that the parabolic (*26*) model well describes our upper bound dynamic behavior, but the MYEGA model (*20*) does not. These results are consistent with the amber work (*9*). It is worth noting that the comparisons here were made to show that the approach of making measurements of the upper bound relaxation times using extremely low fictive temperature glasses will be able to be used to distinguish among nondiverging models in a straightforward fashion. Future work should be undertaken to investigate the effects of molecular structure on the apparent activation energies of the materials below T_g in much the same way as dynamic fragility has been investigated for the above-T_g dynamics of different classes of glass-forming materials.

We have performed viscoelastic measurements on a vapor pyrolysis–formed ultrastable amorphous Teflon in the regime between T_f and T_g. By using the TTU nanobubble inflation creep methodology, we were able to make measurements on the microgram quantities of material made by the very slow vapor deposition method. The results show that the temperature dependence of the dynamics strongly deviates from the classic VFT behavior and toward a high activation energy Arrhenius-like behavior. This strong deviation is consistent with results from prior work for a 20 Ma old amber (*9*). By also comparing the results with two nondiverging models from the literature (*20*, *26*), the approach of testing extremely low fictive temperature glasses in the region between T_f and T_g provides a means to discriminate not only between the data and the VFT extrapolation but also among theories that show nondiverging dynamics. The current results challenge theories and predictions of diverging dynamic behavior above absolute zero and often attributed to an ideal glass transition (*1*, *19*, *21*–*23*, *29*–*32*, *34*). The possibility is that these materials can be used to systematically investigate the deep glassy state and interrogate material behavior in a wider temperature range, thus interrogating the "unexplored" regions of the deep glassy state (*1*).

MATERIALS AND METHODS

Sample preparation

The ultrastable amorphous Teflon films were produced by VPD (*4*, *7*). The weight-average molecular weights for the virgin and VPD amorphous Teflon were 500,000 and 100,000 g/mol, respectively (*7*). The reduced molecular weight for the VPD films was attributed to thermal degradation during the VPD process, including a repolymerization step (*7*). Details are provided in (*7*). Here, 110- to 200-nm-thick amorphous Teflon films were deposited onto mica sheets. During the deposition, the substrate temperature was maintained at 0.85 T_g, and the deposition rate was set to 0.1 nm/s. The T_f was measured by flash DSC. The T_f for the stable glass was 75°C, and that for the rejuvenated sample was 130°C.

Nanobubble inflation

The method is an extension of the classic membrane inflation test (*41*, *42*) to nanometric thin films deposited onto filter templates having micrometer size through channels. The filter templates had 10- and 20-μm-diameter channels in the current study. The 20-μm templates were used for temperatures below 110°C and for the 200-nm-thick film because of the high stiffnesses of the films. Detailed procedures for the creep compliance analysis are described elsewhere (*41*, *42*). The inflated bubbles were monitored using an atomic force microscope, and the creep response was obtained by measuring the bubble radius as a function of time at constant pressure. The nanobubble inflation measurements were performed by following the O'Connell and McKenna (*41*) bubble inflation procedures. The creep experiments were performed for temperatures ranging from 63° to 135°C, following Struik's protocol (fig. S1) (*5*).

A comment here is that the film at 63°C was very stiff, with the result that the heights of the inflated bubbles did not reach the membrane regime that requires a minimum bubble height of three times the film thickness to apply the membrane approximation. Prior bubble inflation studies (*41*, *42*) report that the bending energy needs to be included in the analysis when the bubble heights are less than three times the film thickness. In Fig. 2A, the creep compliances at 63°C were calculated by membrane analysis; hence, the actual compliance would be lower than that calculated from the membrane analysis. However, the purpose of the experiments at 63°C is to show the aging response rather than the absolute creep compliance, which we could not obtain at this low temperature and high material stiffness. The results illustrate that aging occurs but the quantitative aspects are only approximate. Except for the 63°C data, the heights of all the bubbles in the current work were in the membrane regime. In addition, we also note that 63°C was the lowest temperature of the current experiments.

SUPPLEMENTARY MATERIALS

Supplementary material for this article is available at http://advances.sciencemag.org/cgi/content/full/4/12/eaau5423/DC1

Section S1. Struik's protocol

Section S2. Mixing rule

Section S3. Comparison of rejuvenated and ultrastable glass at 105°C

Fig. S1. Schematic diagram for Struik's protocol (*5*) as implemented in this work.

Fig. S2. Creep compliance master curves for vapor-deposited and rejuvenated amorphous Teflon films at 105°C.

REFERENCES AND NOTES

1. G. B. McKenna, S. L. Simon, 50th Anniversary Perspective: Challenges in the dynamics and kinetics of glass-forming polymers. *Macromolecules* **50**, 6333–6361 (2017).
2. G. B. McKenna, J. Zhao, Accumulating evidence for non-diverging time-scales in glass-forming fluids. *J. Non. Cryst. Solids* **407**, 3–13 (2015).
3. G. B. McKenna, Glass dynamics: Diverging views on glass transition. *Nat. Phys.* **4**, 673–674 (2008).
4. M. D. Ediger, Perspective: Highly stable vapor-deposited glasses. *J. Chem. Phys.* **147**, 210901 (2017).
5. L. C. E. Struik, *Physical Aging in Polymers and Other Amorphous Materials* (Elsevier, 1976).
6. S. F. Swallen, K. L. Kearns, M. K. Mapes, Y. S. Kim, R. J. McMahon, M. D. Ediger, T. Wu, L. Yu, S. Satija, Organic glasses with exceptional thermodynamic and kinetic stability. *Science* **315**, 353–356 (2007).
7. H. Yoon, Y. P. Koh, S. L. Simon, G. B. McKenna, An ultrastable polymeric glass: Amorphous fluoropolymer with extreme fictive temperature reduction by vacuum pyrolysis. *Macromolecules* **50**, 4562–4574 (2017).
8. P. A. O'Connell, G. B. McKenna, Arrhenius-type temperature dependence of the segmental relaxation below T_g. *J. Chem. Phys.* **110**, 11054–11060 (1999).
9. J. Zhao, S. L. Simon, G. B. McKenna, Using 20-million-year-old amber to test the super-Arrhenius behavior of glass-forming systems. *Nat. Commun.* **4**, 1783 (2013).
10. J. Zhao, G. B. McKenna, Temperature divergence of the dynamics of a poly (vinylacetate) glass: Dielectric vs. mechanical behaviors. *J. Chem. Phys.* **136**, 154091 (2012).
11. S. L. Simon, J. W. Sobieski, D. J. Plazek, Volume and enthalpy recovery of polystyrene. *Polymer* **42**, 2555–2567 (2001).
12. C. A. Angell, K. L. Ngai, G. B. McKenna, P. F. McMillan, S. W. Martin, Relaxation in glass forming liquids and amorphous solids. *J. Appl. Phys.* **88**, 3113–3157 (2000).
13. F. Stickel, E. W. Fischer, R. Richert, Dynamics of glass-forming liquids. I. Temperature-derivative analysis of dielectric relaxation data. *J. Chem. Phys.* **102**, 6251–6257 (1995).
14. C. T. Moynihan, A. J. Easteal, M. A. De bolt, J. Tucker, Dependence of the fictive temperature of glass on cooling rate. *J. Am. Ceram. Soc.* **59**, 12–16 (1976).
15. A. Q. Tool, Effect of heat-treatment on the density and constitution of high-silica glasses of the borosilicate type. *J. Am. Ceram. Soc.* **31**, 177–186 (1948).
16. M. Goldstein, Viscous liquids and the glass transition: A potential energy barrier picture. *J. Chem. Phys.* **51**, 3728–3739 (1969).
17. F. H. Stillinger, A topographic view of supercooled liquids and glass formation. *Science* **267**, 1935–1939 (1995).
18. P. G. Debenedetti, F. H. Stillinger, Supercooled liquids and the glass transition. *Nature* **410**, 259–267 (2001).
19. G. Adam, J. H. Gibbs, On the temperature dependence of cooperative relaxation properties in glass-forming liquids. *J. Chem. Phys.* **43**, 139–146 (1965).
20. J. C. Mauro, Y. Yue, A. J. Ellison, P. K. Gupta, D. C. Allan, Viscosity of glass-forming liquids. *Proc. Natl. Acad. Sci. U.S.A.* **106**, 19780–19784 (2009).
21. J. H. Gibbs, E. A. DiMarzio, Nature of the glass transition and the glassy state. *J. Chem. Phys.* **28**, 373–383 (1958).
22. A. K. Doolittle, Studies in Newtonian flow. I. The dependence of the viscosity of liquids on temperature. *J. Appl. Phys.* **22**, 1031–1035 (1951).
23. E. A. Di Marzio, A. J. M. Yang, Configurational entropy approach to the kinetics of glasses. *J. Res. Natl. Inst. Stand. Technol.* **102**, 135–137 (1997).
24. V. Lubchenko, P. G. Wolynes, Theory of structural glasses and supercooled liquids. *Annu. Rev. Phys. Chem.* **58**, 235–266 (2007).
25. J. Dudowicz, K. F. Freed, J. F. Douglas, Generalized entropy theory of polymer glass formation. *Adv. Chem. Phys.* **137**, 125–222 (2008).
26. Y. S. Elmatad, D. Chandler, J. P. Garrahan, Corresponding states of structural glass formers. *J. Phys. Chem. B* **113**, 5563–5567 (2009).
27. S. Mirigian, K. S. Schweizer, Elastically cooperative activated barrier hopping theory of relaxation in viscous fluids. II. Thermal liquids. *J. Chem. Phys.* **140**, 194507 (2014).
28. L. A. G. Gray, C. B. Roth, Stability of polymer glasses vitrified under stress. *Soft Matter* **10**, 1572–1578 (2014).
29. H. Vogel, The law of the relation between the viscosity of liquids and the temperature. *Phys. Z.* **22**, 645–646 (1921).
30. G. S. Fulcher, Analysis of recent measurements of the viscosity of glasses. *J. Am. Ceram. Soc.* **8**, 339–355 (1925).
31. G. Tammann, W. Hesse, The dependence of viscosity upon the temperature of supercooled liquids. *Z. Anorg. Allg. Chem.* **156**, 254–257 (1926).
32. W. Kauzmann, The nature of the glassy state and the behavior of liquids at low temperatures. *Chem. Rev.* **43**, 219–256 (1948).
33. A. J. Kovacs, "Transition vitreuse dans les polymères amorphes. Etude phénoménologique." *Fortschritte Der Hochpolymeren-Forschung* **3**, 394–507 (1964).
34. M. L. Williams, R. F. Landel, J. D. Ferry, The temperature dependence of relaxation mechanisms in amorphous polymers and other glass-forming liquids. *J. Am. Chem. Soc.* **77**, 3701–3707 (1955).
35. P. W. Anderson, Through the glass lightly. *Science* **267**, 1615–1616 (1995).
36. T. Hecksher, A. I. Nielsen, N. B. Olsen, J. C. Dyre, Little evidence for dynamic divergences in ultraviscous molecular liquids. *Nat. Phys.* **4**, 737–741 (2008).
37. R. Richert, Comment on "Temperature divergence of the dynamics of a poly (vinylacetate) glass: Dielectric vs. mechanical behaviors". [J. Chem. Phys. 136, 154901 (2012)]. *J. Chem. Phys.* **139**, 137101 (2013).
38. D. Cangialosi, V. M. Boucher, A. Alegrı'a, J. Colmenero, Direct evidence of two equilibration mechanisms in glassy polymers. *Phys. Rev. Lett.* **111**, 095701 (2013).
39. E. A. A. Pogna, C. Rodríguez-Tinoco, G. Cerullo, C. Ferrante, J. Rodríguez-Viejo, T. Scopigno, Probing equilibrium glass flow up to exapoise viscosities. *Proc. Natl. Acad. Sci. U.S.A.* **112**, 2331–2336 (2015).
40. J. Zhao, E. Ragazzi, G. B. McKenna, Something about amber: Fictive temperature and glass transition temperature of extremely old glasses from copal to triassic amber. *Polymer* **54**, 7041–7047 (2013).
41. P. A. O'Connell, G. B. McKenna, Novel nanobubble inflation method for determining the viscoelastic properties of ultrathin polymer films. *Rev. Sci. Instrum.* **78**, 013901 (2007).
42. H. Yoon, G. B. McKenna, "Rubbery stiffening" and rupture behavior of freely standing nanometric thin PIB films. *Macromolecules* **50**, 9821–9830 (2017).
43. D. M. A. Hoffman, A. L. Shields, Rheological properties and molecular weight distributions of four perfluorinated thermoplastic polymers. *Polym. Prepr.* **50**, 156 (2009).
44. M. Alcoutlabi, G. B. McKenna, Effects of confinement on material behavior at the nanometre size scale. *J. Phys. Condens. Matter* **17**, R461–R524 (2005).

Acknowledgments: The authors acknowledge the National Science Foundation under grants DMR-207070 and DMR-1610495 and the John R. Bradford Endowment at TTU, each for partial support of this work. The Office of Naval Research through the DURIP program grant no. N00014-12-1-0876 is also thanked for instrumental support. **Author contributions:** H.Y. performed the experiments to make vapor-deposited amorphous Teflon films, determined the fictive temperatures, and made the nanobubble inflation creep measurements. He analyzed the data and jointly wrote the manuscript. G.B.M. originally conceived of the experiments, mentored H.Y. in his research activities, and worked with H.Y. in the editing and finalizing of the manuscript. **Competing interests:** The authors declare that they have no competing interests. **Data and materials availability:** All data needed to evaluate the conclusions in the paper are present in the paper and/or the Supplementary Materials. Additional data related to this paper may be requested from the authors.

Submitted 20 June 2018
Accepted 20 November 2018
Published 21 December 2018
10.1126/sciadv.aau5423

Citation: H. Yoon, G. B. McKenna, Testing the paradigm of an ideal glass transition: Dynamics of an ultrastable polymeric glass. *Sci. Adv.* **4**, eaau5423 (2018).

ScienceAdvances

Testing the paradigm of an ideal glass transition: Dynamics of an ultrastable polymeric glass

Heedong Yoon and Gregory B. McKenna

Sci Adv **4** (12), eaau5423.
DOI: 10.1126/sciadv.aau5423